Local and Nonlocal Parallel Heat Transport in General Magnetic Fields

D. del-Castillo-Negrete and L. Chacón

Phys. Rev. Lett. **106**, 195004 — Published 11 May 2011

DOI: 10.1103/PhysRevLett.106.195004

Local and nonlocal parallel heat transport in integrable and chaotic magnetic fields

D. del-Castillo-Negrete* and L. Chacón

Oak Ridge National Laboratory

Oak Ridge TN, 37831-8071

Abstract

A novel approach that enables the study of purely parallel transport in magnetized plasmas is presented. The method avoids numerical pollution issues of standard grid-based formulations, and applies to general 3D magnetic fields with either local or nonlocal parallel closures. The method is applied to study radial heat transport in cylindrical geometry with unbounded field lines. In weakly chaotic fields, the method gives the fractal structure of the Devil's staircase radial temperature profile. In fully chaotic fields, the temperature exhibits self-similar spatio-temporal evolution characterized by a stretched exponential scaling function for local closures, and by an algebraically decaying one for non-local closures. In both cases, the computation of the flux and the gradient shows that the effective radial heat transport is incompatible with the quasilinear diffusion transport model.

*Electronic address: `delcastillod@ornl.gov`

The study of transport in magnetized plasmas is a problem of fundamental interest in controlled fusion, space plasmas, and astrophysics research. Three issues make this problem particularly challenging: (i) The *extreme anisotropy* between the parallel (i.e., along the magnetic field), $\chi_\parallel$, and the perpendicular, $\chi_\perp$, conductivities ($\chi_\parallel/\chi_\perp$ may exceed 10^{10} in fusion plasmas); (ii) Magnetic *field lines chaos* which in general complicates (and may preclude) the construction of magnetic field line coordinates; and (iii) *Nonlocal parallel transport* in the limit of small collisionality. As a result of these challenges, standard finite-difference and finite-element numerical methods suffer from a number of ailments. Chief among them are the pollution of perpendicular dynamics due to truncation errors in the discrete representation of the parallel heat flux, and the lack of a discrete maximum principle (to enforce temperature positivity). In addition to these accuracy challenges, potentially insurmountable issues exist regarding the algorithmic inversion of the discretized transport equation. In particular, depending on boundary conditions, the continuum parallel transport operator may feature a finite (and potentially degenerate) null space [1]. In the discrete, and owing to numerical pollution, the otherwise strictly zero eigenvalues of the null space may give way to arbitrarily small eigenvalues in the associated matrix, which might render the use of modern iterative inversion methods (e.g., Krylov methods) impractical.

Despite the severity of these issues, recent studies have succeeded in partially addressing some of them, and important progress has been made in the study of parallel transport. Reference [2] discusses a finite-element numerical implementation of nonlocal heat transport with applications including temperature flattening across magnetic islands and tokamak disruptions. The use of high-order discretizations has been shown to mitigate numerical pollution of the perpendicular dynamics in finite-difference [3, 4] and finite-element methods [4, 5]. A maximum principle has been shown to be enforceable by the use of limiters at the discrete level in finite differences [6] and finite elements [7], albeit with the effect of rendering both spatial discretizations formally first-order accurate. Steady-state solutions for anisotropic heat transport in chaotic magnetic fields were determined numerically and compared with the so-called "ghost surfaces" in Refs. [8, 9].

Motivated by the strong anisotropy typically encountered in magnetized plasmas ($\chi_\parallel/\chi_\perp \sim 10^{10}$), we study parallel heat transport in the extreme anisotropic regime $\chi_\perp = 0$. To overcome the numerical and algorithmic challenges discussed above, we present a novel Lagrangian Green's function approach. The proposed method bypasses the need to discretize and invert the transport operators on a grid and allows the integration of the parallel transport equation without perpendicular pollution, while preserving the positivity of the temperature field at all times. The method is applicable to local and non-local transport in integrable or chaotic magnetic fields.

As an application of the proposed method, we study radial heat transport in cylindrical geometry in the presence of weakly chaotic and fully chaotic magnetic fields. The weakly chaotic case is presented to illustrate the accuracy of our method (which in the case of purely parallel transport provides a pollution-free solution of the radial temperature at any radial scale). Reference [8] showed that, for large $\chi_\parallel/\chi_\perp$, the radial temperature profile approaches a Devil's staircase. Here, going beyond previous studies, we unveil the fractal structure of the Devil's staircase in the previously unaccessible $\chi_\perp = 0$ regime. This result opens the possibility of a deeper understanding of the role of Cantori which have been observed to act as partial transport barriers in numerical studies [8, 9] and experiments [10]. The second application pertains the study of heat transport in fully chaotic fields. This has been a problem of considerable interest in fusion and astrophysical plasmas since the pioneering work in Refs. [11, 12]. Here, we present novel results concerning the self-similar spatio-temporal evolution of the radial temperature profile. Most importantly, we show that, contrary to what is typically assumed in transport studies, the effective radial transport of temperature is not diffusive. In particular, transport does not adhere to the Fourier-Fick's prescription that assumes a local linear relation between the radial heat flux and the radial temperature gradient.

Our starting point is the heat transport equation in a constant-density plasma

$$\partial_t T = -\nabla \cdot \mathbf{q}\,, \tag{1}$$

where $\mathbf{q}$ is the heat flux. For local transport, in the limit $\chi_\perp = 0$,

$$\mathbf{q} = -\chi_\parallel \left[\hat{\mathbf{b}} \cdot \nabla T\right] \hat{\mathbf{b}}\,, \tag{2}$$

where $\hat{\mathbf{b}} = \mathbf{B}/|B|$. Substituting (2) into (1), we get

$$\partial_t T = -\partial_s q_\parallel\,, \qquad q_\parallel = -\chi_\parallel \partial_s T\,, \tag{3}$$

where $\partial_s = \hat{\mathbf{b}} \cdot \nabla$ is the derivative along the field line, and we have assumed the tokamak ordering $\partial_s \ln B \approx 0$. For non-local transport, we follow Refs. [2, 13, 14] and consider the closure

$$q_{\|} = -\frac{\chi_{\|}}{\pi} \int_0^{\infty} \frac{T(s+z) - T(s-z)}{z} dz \,. \tag{4}$$

In Fourier space, both transport models can be written in the particularly compact form

$$\partial_t \hat{T} = -\chi_{\|} |k|^{\alpha} \hat{T} \,, \tag{5}$$

where $\hat{T}$ is the Fourier transform of T. For the local closure in Eq. (3), $\alpha = 2$, whereas for the non-local closure in Eq. (4), $\alpha = 1$. In principle, $\chi_{\|}$ can have a spatial dependence, but it must be constant along field lines, i.e. $\partial_s \chi_{\|} = 0$. This assumption is not overly restrictive when one is interested in the long-term asymptotic regime (the case in this study), as the steady-state solution of Eq. (1) is a constant temperature along magnetic field lines.

The proposed method is based on the Green's function solution of Eq. (5) along the magnetic field. The unique magnetic field line trajectory, $\mathbf{r}(s)$ (parametrized by the arc length s) that goes through a point $\mathbf{r}_p$ is given by the solution of

$$\frac{d\mathbf{r}}{ds} = \hat{\mathbf{b}} \,, \qquad \mathbf{r}(s=0) = \mathbf{r}_p \,. \tag{6}$$

Thus, given an initial condition in the whole domain, $T(\mathbf{r}, t=0)$, the temperature at $\mathbf{r} = \mathbf{r}_p$ at time t is given by

$$T(\mathbf{r}_p, t) = \int_{s_1}^{s_2} T_0 \left[\mathbf{r}(s)\right] G_{\alpha}(s,t) ds \,, \tag{7}$$

where $T_0[\mathbf{r}(s)] = T[\mathbf{r}(s), t=0]$ is the initial condition along the field line. G_{α} is the Green's function defined as the solution of the initial value problem of Eq. (5) for a Dirac delta function initial condition in space. For unbounded field lines $[(s_1, s_2) = (-\infty, \infty)]$, the Green's function is given by

$$G_{\alpha}(s,t) = \frac{1}{2\pi} \int_{-\infty}^{\infty} e^{-\chi_{\|} t |k|^{\alpha} - iks} dk \,. \tag{8}$$

For $\alpha = 2$ (local transport), Eq. (8) gives the Gaussian distribution

$$G_2(s,t) = \frac{1}{2\sqrt{\pi}} \left(\chi_{\|} t\right)^{-1/2} \exp\left[-\frac{s^2}{4\chi_{\|} t}\right] \,, \tag{9}$$

and for $\alpha = 1$ (non-local, free-streaming transport), it gives the Cauchy distribution

$$G_1(s,t) = \frac{\left(\chi_{\|} t\right)^{-1}}{\pi} \frac{1}{1 + \left(s/\chi_{\|} t\right)^2} \,. \tag{10}$$

The main advantage to use the free-streaming non-local closure in Eq. (4) is the existence of the analytically tractable Green's function in Eq. (10). However, more general closures, like those in Refs. [2, 14], are straightforward to implement by first computing the Green's function numerically. It is also interesting to point out that, for non-integer $1 < \alpha < 2$, the Green's function in Eq. (8) is $G_\alpha = (\chi_\parallel t)^{-1/\alpha} K_{\alpha,0}[(\chi_\parallel t)^{-1/\alpha} s]$, where $K_{\alpha,0}$ is the symmetric α-stable Levy distribution [15]. In what follows, we limit attention to unbounded field lines. However, transport along bounded lines including periodic lines in two and three dimensions or lines intersecting boundaries can also be studied with the appropriate Green's function. The numerical integration of the field-line trajectories in Eq. (6) was done using the high-order adaptive ODE solver ODEPACK. In the numerical evaluation of Eq. (7) for unbounded field lines, the integration limits were truncated to a finite value that guaranteed the error to remain below a specific relative tolerance (10^{-5} for the results reported here). We have thoroughly verified the numerical implementation against analytical solutions.

At this point, it is important to indicate a fundamental difference between our work and the numerical implementation of the nonlocal closure discussed in Refs. [2, 14]. In these references, the flux is calculated by integrating the transport kernel along the field lines. But, once the flux is computed, the Lagrangian approach is abandoned and the flux is mapped to Gaussian quadrature points for the finite-element standard integration of the temperature evolution equation on a grid. In contrast, in the method proposed here, the assumption $\chi_\perp = 0$ allows the use of a fully Lagrangian approach that completely bypasses the use of finite differences or finite elements, thus circumventing the numerical issues discussed earlier.

In what follows, we apply the Lagrangian Green's function method to study local and non-local parallel transport in weakly and fully chaotic 3-D magnetic fields. We assume a periodic, straight cylinder configuration of length $L = 2\pi R$ with $R = 5$. The magnetic field consists of a perturbed tokamak-like equilibrium of the form

$$\mathbf{B} = (rB/\lambda)/[1 + (r/\lambda)^2]\hat{\mathbf{e}}_\theta + B_0\hat{\mathbf{e}}_z + \mathbf{B}_1(r, \theta, z)\,. \tag{11}$$

The radial dependence on the equilibrium field is chosen to model a monotonically increasing safety factor, q, which is common in standard tokamak operations.The perturbation $\mathbf{B}_1$ can be due to imperfections in the coils, or due to slow magnetohydrodynamic activity which for the purpose of fast parallel transport can be assumed time independent. The magnetic field has been normalized to the amplitude of the equilibrium toroidal component, i.e., $B_0 = 1$.

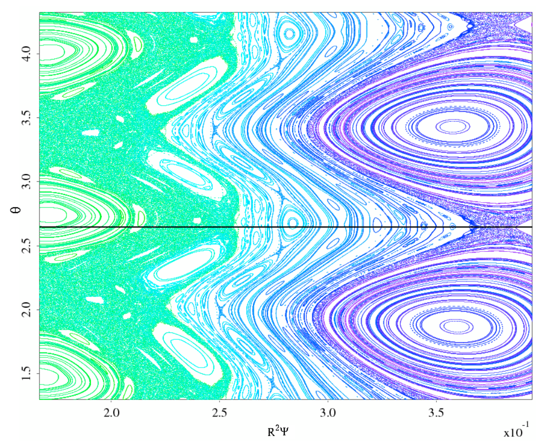

FIG. 1: Poincare plot of the weakly chaotic magnetic field used in the solution of the parallel heat transport equation shown in Fig. 2.

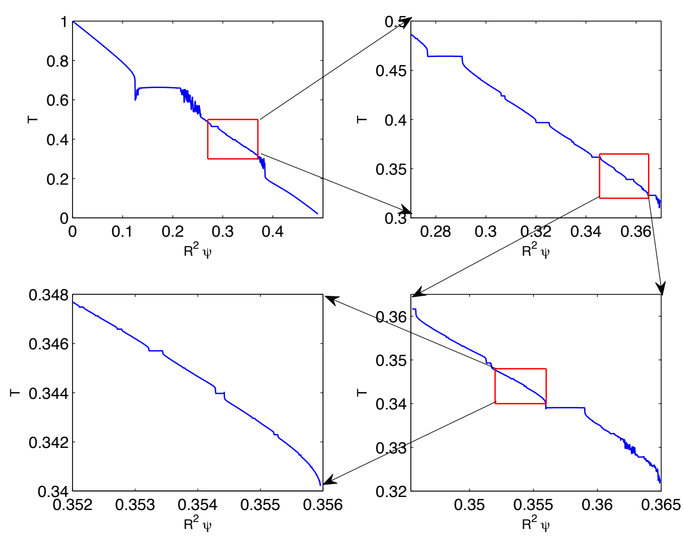

FIG. 2: Radial temperature profile of the time-asymptotic solution of the parallel heat transport equation for the weakly chaotic magnetic field in Fig. 1. The zooms in the successive panels unveil the fractal structure of the Devil's staircase profile.

Consistent with the tokamak ordering, we choose B so that $B/B_0 = 10^{-1}$. To fit a spectrum of resonant modes with n/m ranging from 4/5 to 1/5, we choose λ so that $q_{min} = 1.24 \approx 5/4$ and $q_{max} = 5$. The magnetic potential of the perturbation, $\mathbf{B}_1 = \nabla \times A_z \hat{\mathbf{e}}_z$, consists of a superposition of modes

$$A_z(r, \theta, z) = \sum_{m,n} A_{mn}(r) \cos\left(m\theta - nz/R + \zeta_{mn}\right) , \tag{12}$$

with

$$A_{mn} = \epsilon a(r) \left(\frac{r}{r_*}\right)^m \exp\left[\left(\frac{r_* - r_0}{\sqrt{2}\sigma}\right)^2 - \left(\frac{r - r_0}{\sqrt{2}\sigma}\right)^2\right], \tag{13}$$

$\epsilon = 10^{-4}$, and $\sigma = 0.5$. For each (m, n), the values of r_* and r_0 are chosen so that the safety factor satisfies $q(r_*) = m/n$ and $dA_{mn}/dr(r = r_*) = 0$. The prefactor $(r/r_*)^m$ is included to guarantee the regularity of the radial eigenfunction near the origin, $r \sim 0$. The function, $a(r) = \{1 - \tanh[(r-1)/0.05]\}/2$, is introduced to guarantee the perturbation to vanish at $r = 1$ and thus the existence of well-defined flux surfaces at the plasma boundary.

In the study of transport in weakly chaotic fields, only two modes $(m, n) = (5, 2), (4, 1)$ were included. As the Poincare plot in Figure 1 shows, in this case the magnetic field exhibits a rich fractal-like structure resulting from the existence of higher-order resonances. In this and all the subsequent results, $\psi = r^2/(2R^2)$ denotes the radial flux coordinate. As discussed in Ref.[8, 9, 16], weakly chaotic fields give rise to Devil's staircase temperature profiles in which higher-order resonances lead to flat spots in the profile, while KAM invariant circles and Cantori lead to strong gradients. Our numerical method is able to find an accurate solution of the radial temperature profile at arbitrary radial resolutions. To illustrate this, we show in Fig. 2 the fractal structure of Devil's staircase in the previously unaccessible limit $\chi_\parallel/\chi_\perp \to \infty$. The plots shows the time asymptotic, radial temperature profile along the $\theta = 2.7$ horizontal line in Fig. 1, corresponding to the initial condition $T_0 = 1 - 2R^2\psi$. Note that the steady state is the same in the local and the non-local cases. This is because, asymptotically, both transport operators enforce constant temperature along field lines.

To study transport in a fully chaotic magnetic field, we consider a set of twenty one strongly overlapping modes. In this case, the Poincare plot (not shown) is fully hyperbolic and does not exhibit any structure. The initial condition consists of a narrow "cylindrical shell" of the form $T_0 = \exp[-R^2(\psi - \psi_0)^2/\sigma^2]$, with $\psi_0 = 0.18$ and $\sigma = 0.05$. Figure 3 shows the time evolution of the radial profile of the temperature averaged in θ and z, $\langle T \rangle$, in the local and the non-local (free-streaming) regimes. In both regimes, the temperature exhibits an asymptotic self-similar evolution of the form

$$\langle T \rangle(\psi, t) = \left(\chi_\parallel t\right)^{-\gamma/2} L(\eta), \tag{14}$$

where the similarity variable is defined as $\eta = (\psi - \psi_0)/(\chi_\parallel t)^{\gamma/2}$, with γ the scaling exponent. From here, it follows that the second moment scales as $\overline{\psi^2} \sim t^\gamma$. Consistently with Refs. [11, 12], we find sub-diffusive scaling ($\gamma = 1/2$) in the case of local transport ($\alpha = 2$), and

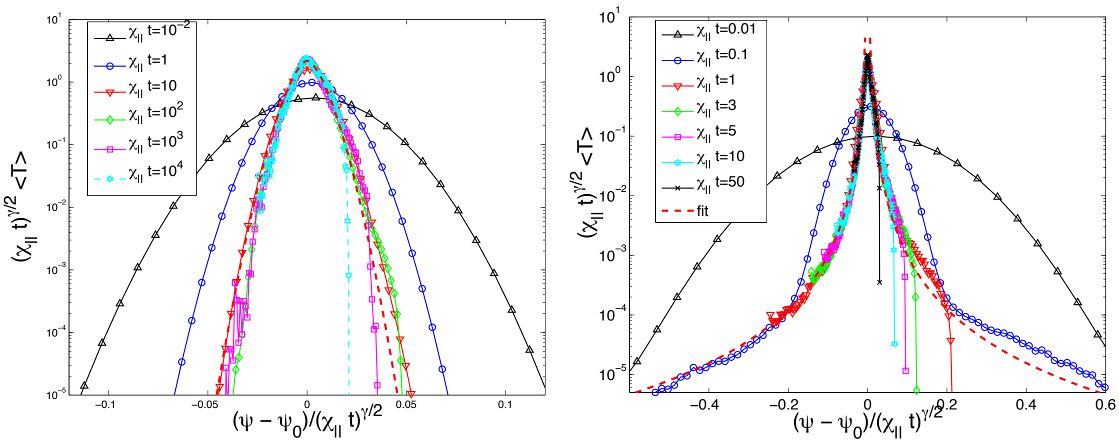

FIG. 3: Self-similar spatio-temporal evolution of the radial temperature profile in a fully chaotic magnetic field. The left panel shows the local transport ($\alpha = 2$) case with sub-diffusive scaling exponent $\gamma = 1/2$. The dashed line denotes a stretched exponential fit $L \sim \exp\left[-\left(|\eta|/\mu\right)\right)^{\nu}]$ with $\nu \approx 1.6$ and $\mu \approx 0.0095$. The right panel shows the non-local transport ($\alpha = 1$) case with diffusive scaling exponent $\gamma = 1$. In this case, the scaling function is strongly non-Gaussian and, as the dashed-line fit shows, it exhibits algebraic decay of the form $L \sim \eta^{-3}$.

diffusive scaling ($\gamma = 1$) in the case of free streaming ($\alpha = 1$). However, the study of the properties of the scaling function provides important transport information beyond the scaling of the second moment. As Fig. 3 shows, for local parallel transport the scaling function can be fitted by an stretched-exponential of the form $L \sim \exp\left[-\left(|\eta|/\mu\right)\right)^{\nu}]$, with $\nu \approx 1.6$ and $\mu \approx 0.0095$. In contrast, the scaling function in the nonlocal case is strongly non-Gaussian and exhibits an algebraic decay of the form $L \sim \eta^{-3}$.

A key issue in the study of heat transport in magnetically confined plasmas is to understand the effective radial energy transport, which ultimately determines the energy confinement time of the system. Within the standard diffusion paradigm, the study of radial transport is based on the Fourier-Fick's prescription. This prescription assumes that the the radial heat flux and the radial temperature gradient, averaged over z and θ, satisfy $\langle \mathbf{q} \cdot \hat{e}_\psi \rangle = -\chi_{eff} \langle \nabla T \cdot \hat{e}_\psi \rangle$, where $\hat{e}_\psi = \hat{e}_r$ is the unit vector in the radial direction. Although this prescription is used to model a wide range of transport problems, recent studies have questioned its validity in the presence of non-diffusive and non-local transport phenomena (see for example Ref. [15, 17, 18] and references therein). In fact, in what follows, we show that, unless one incorporates unphysical spatio-temporal dependencies in χ_{eff}, the effective radial heat transport resulting from parallel transport in fully stochastic 3-D magnetic fields is inconsistent with the local diffusion assumption. Our approach is based on the comparison between the temperature gradient $\langle \nabla T \cdot \hat{e}_\psi \rangle$ and the heat flux $\langle \mathbf{q} \cdot \hat{e}_\psi \rangle$, both of which are computed directly from the solutions $\langle T \rangle$ of the parallel heat transport equation shown in Fig. 3. The flux as a function of ψ is obtained from

$$\langle \mathbf{q} \cdot \hat{e}_\psi \rangle = -\frac{1}{\sqrt{2\psi}} \frac{d}{dt} \int_0^\psi \langle T \rangle d\psi' \,, \tag{15}$$

which follows from Eq. (1), and the gradient $\langle \nabla T \cdot \hat{e}_\psi \rangle = \sqrt{2\psi}\, \partial_\psi \langle T \rangle$. Figure 4 shows the parametric curves $\mathcal{C}(\psi) = [-\langle \nabla T \cdot \hat{e}_\psi \rangle(\psi), \langle \mathbf{q} \cdot \hat{e}_\psi \rangle(\psi)]$ tracing the values of the flux and the gradient as functions of ψ in the flux-gradient plane. In both the diffusive $\alpha = 2$ and the free-streaming $\alpha = 1$ cases, the flux-gradient parametric curves exhibit two key features: (i) the flux is a multivalued function of the gradient (i.e. the curves exhibit "loops") and (ii) the shape of the curves depends on time. In the case of a constant (in space and time) diffusivity χ_{eff}, the local diffusion assumption requires the parametric curves to be straight lines. The only way to make the local diffusion assumption consistent with a multivalued flux-gradient relation is to incorporate an *ad hoc* spatial dependence in χ_{eff}. Similarly, the only way to explain the temporal variation of the flux-gradient curves is to incorporate an *ad hoc* temporal dependence in χ_{eff}. Although, formally, one could construct these spatio-temporal diffusivities to fit the data, such dependencies are inconsistent with the physics of the problem because the magnetic field is time-independent, and the field-line chaos is uniform in ψ by construction.

Summarizing, in this Letter we have proposed a Lagrangian Green's function method for the accurate and efficient computation of purely parallel ($\chi_\perp = 0$) local and non-local transport in arbitrary 3-D magnetic fields. Because of the parallel nature of the Lagrangian calculation, the formulation naturally leads to a massively parallel implementation, suitable for today's supercomputers. The numerical capabilities of the method and its accuracy properties have been demonstrated by computing the fractal (Devil's staircase) temperature profile in weakly chaotic fields in the previously unaccessible, $\chi_\perp = 0$, case. We have also solved the parallel heat transport equation in a fully chaotic field and showed that the radial temperature profile exhibits spatio-temporal self-similarity with non-diffusive scaling functions (stretched exponential in the case of local closures, and algebraically decaying ones in the case of non-local closures). Most importantly, our computation of the flux and the

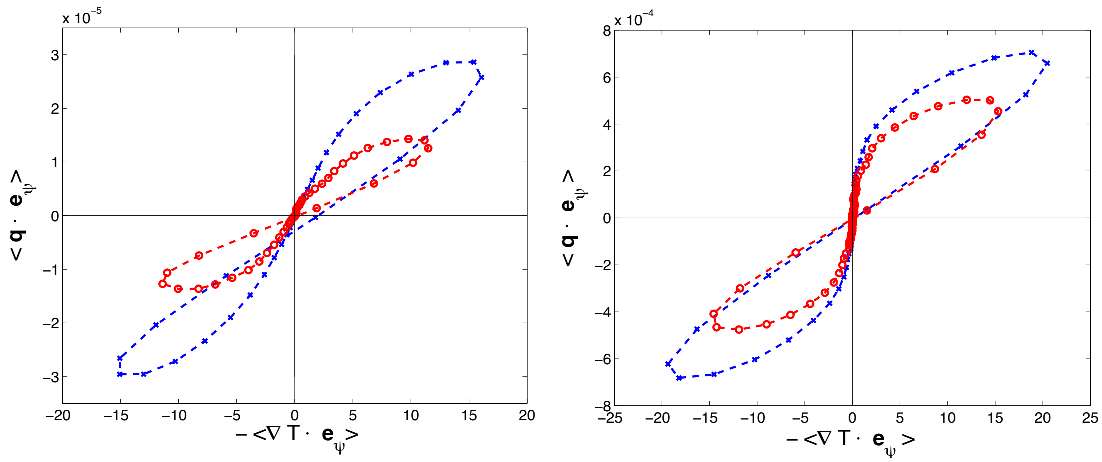

FIG. 4: Flux-gradient parametric curves obtained from the numerical integration of the parallel heat transport equation in a fully chaotic magnetic field. The left panel corresponds to the local transport ($\alpha = 2$) solutions shown in Fig. 3 for $\chi_\| t = 80$ (dashed-crosses line) and $\chi_\| t = 200$ (dashed-circles line). The right panel corresponds to the free-streaming transport ($\alpha = 1$) solutions shown in Fig. 3 for $\chi_\| t = 4$ (dashed-crosses line) and $\chi_\| t = 8$ (dashed-circles line).

gradient showed that the effective radial heat transport is incompatible with the quasilinear diffusion transport model.

I. ACKNOWLEDGMENTS

This work was sponsored by the Office of Applied Scientific Computing Research and the Office of Fusion Energy Sciences of the US Department of Energy at Oak Ridge National Laboratory, managed by UT-Battelle, LLC, for the U.S.Department of Energy under contract DE-AC05-00OR22725.

[1] S. R. Hudson, Phys. Plasmas **17**, 114501 (2010)

[2] E. D. Held, J. D. Callen, C. C. Hegna, C. R. Sovinec, T. A. Gianakon, and S. E. Kruger, Phys. Plasmas, **11**, 2419, (2004).

[3] S. Guenter, Q. Yu, J. Kruger, and K. Lackner, J. Comp. Phys., **209**, 354 (2005).

[4] S. Guenter, K. Lackner, and C. Tichmann, J. Comput. Phys., vol. **226**, 2306–2316 (2007).

[5] C. R. Sovinec, A. H. Glasser, T. A. Gianakon, D. C. Barnes, R. A. Nebel, S. E. Kruger, D. D. Schnack, S. J. Plimpton, A. Tarditi, and M. S. Chu, J. Comput. Phys., vol. **195**, 355–386 (2004).

[6] P. Sharma and G. W. Hammett, J. Comput. Phys., vol. **227**,123–142, (2007).

[7] D. Kuzmin, M. J. Shashkov, and D. Svyatskiy, J. Comput. Phys. vol. **228**, 3448–3463, (2009).

[8] S. R. Hudson and J. Breslau, Phys. Rev. Lett., **100**, 095001 (2008).

[9] S. R. Hudson, Phys. Plasmas, **16**, 010701 (2009).

[10] R. Lorenzini et al., Nature Physics, **5**, 570-574 (2009).

[11] J. R. Jokipii and E. N. Parker, Phys. Rev. Lett., **21**, 44 (1968).

[12] A. B. Rechester and M. N. Rosenbluth, Phys. Rev. Lett., **40**, 38 (1978).

[13] G. W. Hammet and F. W. Perkins, Phys. Rev. Lett., **64**, 3019 (1990).

[14] E. D. Held, J. D. Callen, C. C. Hegna, and C. R. Sovinec, Phys. Plasmas, **8**, 1171, (2001).

[15] D. del-Castillo-Negrete, B.A. Carreras, and V. Lynch, Phys. of Plasmas **11**, 3854 (2004).

[16] S. R. Hudson, Phys. Rev. E, **76**, 046211 (2007).

[17] D. del-Castillo-Negrete, Phys. of Plasmas **13**, 082308 (2006).

[18] D. del-Castillo-Negrete, P. Mantica, V. Naulin, and J. J. Rasmussen, Nucl. Fusion **48**, 075009 (2008).